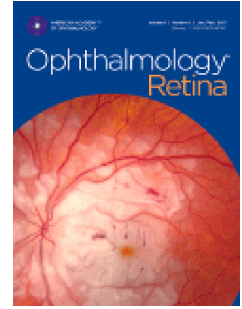# Journal Pre-proof

Juvenile Batten disease (*CLN3*): Detailed Ocular Phenotype, Novel Observations, Delayed Diagnosis, Masquerades, and Prospects for Therapy

Genevieve A. Wright, Michalis Georgiou, Anthony G. Robson, Naser Ali, Ambreen Kalhoro, Kleine Holthaus SM, Nikolas Pontikos, Ngozi Oluonye, Emanuel R. de Carvalho, Magella M. Neveu, Richard G. Weleber, Michel Michaelides

1 **Juvenile Batten disease (*CLN3*): Detailed Ocular Phenotype, Novel**
2 **Observations, Delayed Diagnosis, Masquerades, and Prospects for**
3 **Therapy.**
4

5 Genevieve A. Wright[1,2,4], Michalis Georgiou[1,2,4], Anthony G. Robson[1,2], Naser Ali[1,2,] Ambreen

6 Kalhoro[2], Kleine Holthaus SM [1], Nikolas Pontikos[1,2], Ngozi Oluonye [2], Emanuel R. de

7 Carvalho[2], Magella M. Neveu[1,2], Richard G. Weleber[3], Michel Michaelides[1,2]

8 [1] UCL Institute of Ophthalmology, University College London, London, UK.

9 [2] Moorfields Eye Hospital, London, UK.

10 [3] Casey Eye Institute, Oregon Health & Science University, Portland, Oregon, USA.

11 [4] Contributed equally and should be considered equivalent authors.

12 **Corresponding author**:

13 Michel Michaelides,

14 UCL Institute of Ophthalmology,

15 11-43 Bath Street, London, EC1V 9EL, UK.

16 E-mail: michel.michaelides@ucl.ac.uk

17 Tel. no: 004420 7608 6864

23 **Disclosures:** RG Weleber serves on advisory boards for the Foundation Fighting Blindness.

24 No conflicting relationship exists for any other author.

25 **Running Title:** Juvenile Batten Disease

26 **Abstract (350 words)**

27

28 **Purpose:** To characterize the retinal phenotype of juvenile neuronal ceroid lipofuscinosis

29 (JNCL), highlight delayed and mistaken diagnosis, and propose an algorithm for early

30 identification.

31

32 **Design:** Retrospective case series.

33

34 **Subjects:** Eight children (5 females) with JNCL.

35

36 **Methods:** Review of clinical notes, retinal imaging including fundus autofluorescence (FAF)

37 and optical coherence tomography (OCT), electroretinography (ERG), and both microscopy

38 and molecular genetic testing.

39

40 **Main Outcome Measurements:** Demographic data, signs and symptoms, visual acuity, FAF

41 and OCT findings, ERG phenotype, and microscopy/molecular genetics.

42

43 **Results:**

44 Subjects presented with rapid bilateral vision loss over one to eighteen months, with mean

45 visual acuity deteriorating from 0.44 LogMAR (range: 0.20 - 1.78 LogMAR) at baseline, to

46 1.34 LogMAR (0.30 LogMAR - light perception) at last follow-up. Age of onset ranged from 3

47 to 7 years (mean 5.3 years). The age at diagnosis of JNCL ranged from 7 to 10 years (mean

48 8.3 years). Six children displayed eccentric fixation, and six had cognitive or neurological

49 signs at time of diagnosis (75%). Seven patients had bilateral bull's-eye maculopathy at

50 presentation. Coats-like exudative vasculopathy, not previously reported in JNCL, was

51 observed in one patient. OCT imaging revealed near complete loss of outer retinal layers,

52 and marked atrophy of the nerve fibre and ganglion cell layers, at the central macula. An

53 'electronegative' ERG was present in four patients (50%), but with additional a-wave

54 reduction; there was an undetectable ERG in the remaining four. Blood film microscopy

55 revealed vacuolated lymphocytes and electron microscopy showed lysosomal (fingerprint)

56 inclusions, in all eight patients.

57

58 **Conclusions:**

59 In a young child with bilateral rapidly progressive vision loss and macular disturbance, blood

60 film microscopy to detect vacuolated lymphocytes is a rapid, readily accessible, and

61 sensitive screening test for JNCL. Early suspicion of JNCL can be aided by detailed directed

62 history and high-resolution retinal imaging, with subsequent targeted microscopy/genetic

63 testing. Early diagnosis is critical to ensure appropriate management, counselling, support

64 and social care for children and their families. Furthermore, although potential therapies for

65 this group of disorders are in early phase clinical trial, realistic expectations are that

66 successful intervention will be most effective when initiated at the earliest stage of disease.

67 **Introduction**

68 The neuronal ceroid lipofuscinoses (NCLs) are a group of inherited neurodegenerative

69 lysosomal storage disorders that have been associated with 13 causative genes to date.[1]

70 Prevalence is 1 in 100,000 live births.[2] Traditionally, the disease was divided into different

71 forms dependent on the disease onset. Since disease onset and progression can vary

72 substantially, genetic testing and confirmation of the underlying sequence variant is often

73 required for a definite diagnosis. Consequently, a new gene-based nomenclature was

74 introduced to facilitate disease classification.[3] Classic *CLN3* disease with juvenile disease

75 onset, formerly known as juvenile neuronal ceroid lipofuscinosis (JNCL) and commonly

76 referred to as Batten disease, is a form of NCL caused by sequence variants in the gene *CLN3*

77 (Ceroid Lipofuscinoscis, Neuronal, 3; OMIM: 204200). The gene codes for a transmembrane

78 protein of unknown function.[4, 5] Presentation is typically in early childhood with vision loss

79 at 4-10 years of age, behavioural and cognitive dysfunction (7-10 years), progressive motor

80 decline and seizures (10-13 years), eventually leading to premature death in the

81 second/third decade of life.[6,7] The most common sequence variant in *CLN3* is a homozygous

82 1kb deletion, accounting for approximately 85% of cases of JNCL.[8, 9] This deletion

83 encompasses exons 7-8, resulting in a truncated, non-functional protein.[10] Other variants in

84 *CLN3* can cause isolated adult onset retinal degeneration.[11, 12] Diagnosis of JNCL is confirmed

85 by the presence of vacuolated lymphocytes and lysosomal (fingerprint) inclusions on blood

86 film,[4, 13-15] alongside molecular genetic testing.[3]

87 Visual impairment presents as the first symptom in over 80% of cases of JNCL at a

88 mean age of around 5 years old.[16, 17] Retinal examination often shows a bulls-eye

89 maculopathy, temporal optic disc pallor, peripheral retinal pigment epithelial disturbance

90 (including bone spicule formation) and retinal vascular attenuation.[9, 18-20] In one study,

91   fundus imaging showed widespread atrophy of the retinal pigment epithelium (RPE) in 93%

92   (n=24) of cases of confirmed *CLN3* disease.[21] However, because these retinal findings

93   overlap with selected pathological hallmarks of more common disorders including retinitis

94   pigmentosa, Stargardt disease and other inherited retinal diseases,[22-24] the early diagnosis of

95   JNCL often results in significant diagnostic challenge. Furthermore, one clinical study

96   reported only two out of nine molecularly confirmed *CLN3*-JNCL patients as having bulls-eye

97   maculopathy,[25] and another suggested that only 20% of cases present with a bulls-eye

98   appearance, further highlighting the difficulties in early detection of JNCL.[21] Another less

99   well recognised clinical feature which can be seen in JNCL is "eccentric vision" or

100 "overlooking", whereby the child will raise their eyes to overlook and fixate on a target

101 object, and may be secondary to a relative degree of superior peripheral retinal sparing.[26]

102   The electroretinogram (ERG) is valuable in the diagnostic armamentarium for JNCL,[25]

103 with marked ERG abnormalities invariably seen, including electronegative waveforms.[22, 27, 28]

104 As the disease progresses to more advanced stages the ERG shows significantly reduced

105 cone responses and no recordable rod-specific responses.[18] Cognitive and behavioural

106 impairment, in particular mood, memory and attention (eg inability of the child to recall and

107 accomplish three-step commands), usually appears approximately two years after the onset

108 of visual decline, however these features may be present at first onset or occasionally in

109 advance of visual symptoms; highlighting the importance of careful directed history in

110 suspected cases.[16, 17] Magnetic resonance imaging may show cerebral and cortical atrophy

111 with demyelination.[29]

112   Timely diagnosis of JNCL is often challenging. Given the rapidly progressive and

113 unfavourable prognosis of the disease, early diagnosis is important both to provide timely

114 clinical management and support, and to also prepare for potential novel avenues of

115 intervention. Herein, we describe eight cases of JNCL presenting at a single tertiary referral

116 center in detail, highlighting delayed/mistaken diagnosis, diagnostic challenges, providing

117 diagnostic insights, novel observations and recommendations, and also discuss the latest

118 research avenues being explored and on-going/planned clinical trials.

119 **Materials and Methods**

120 *Patient Identification*

121 Patients with the diagnosis of JNCL and harboring likely disease-causing variants in *CLN3*

122 were identified from the Moorfields Eye Hospital Inherited Eye Disease database. Patients

123 were included in this database after obtaining informed consent. This retrospective

124 study adhered to the tenets of the Declaration of Helsinki and was approved by the

125 Moorfields Eye Hospital ethics committee.

126

127 *Assessment*

128 Medical notes and clinical images were reviewed, including dilated fundoscopy, visual acuity

129 (VA), electrophysiological testing (ERG), and retinal imaging including optical coherence

130 tomography (OCT) and fundus autofluorescence (FAF).

131 The age of disease onset was defined as the age at which the first disease related

132 symptom(s)/sign(s) were apparent. Screening for JNCL was done by microscopic evaluation

133 of a peripheral blood film for the presence of vacuolated lymphocytes; followed by electron

134 microscopy for storage (fingerprint) inclusions. Confirmation of the diagnosis was done by

135 molecular genetic screening for *CLN3* variants.

136 Methods of electrophysiological testing were adapted according to age and the

137 ability of each individual to comply with testing. Full-field electroretinography (ERG) was

138 performed to incorporate the International Society for Clinical Electrophysiology of Vision

139 (ISCEV) standards,[30] using a ganzfeld bowl and gold foil corneal electrodes (case 7) or lower

140 eyelid skin electrodes (case 6). The ERGs in the other children were performed with skin

141 electrodes without mydriasis, using flashes delivered by a Ganzfeld bowl (cases 3, 5, and 8)

7

142 or hand-held strobe (case 4), according to a modified protocol.[31] ISCEV-standard pattern

143 ERG (PERG),[32] was performed using gold foil corneal (case 7) or skin electrodes.

144 The mean subfoveal choroidal thickness was measured by enhanced depth imaging

145 horizontal OCT crosshair scans (EDI-OCT, Heidelberg Engineering Inc., Heidelberg, Germany).

146 Segmentation of macular ganglion cell layer (mGCL) thickness was obtained using the

147 automated segmentation software for the Spectralis OCT device (Heidelberg Engineering,

148 software version 1.10.2.0). For retinal thickness maps, three circular lines representing 1, 3

149 and 6 mm scan diameters (Early Treatment Diabetic Retinopathy Study; ETDRS macula)

150 were obtained. The macular scans were performed in the 30° perifoveal area using a

151 30°×25° OCT volume scan. The average of all points within the inner 1 mm diameter circle

152 was defined as the central subfield thickness. The intermediate 3mm ring was divided into

153 the inner superior, inner nasal, inner inferior and inner temporal subfields and average

154 values were calculated per sector in each eye.

155

156 **Results**

157 *Clinical Findings*

158 All eight ascertained patients were first seen at Moorfields Eye hospital over a period of 8

159 years (2009-2017) and received the diagnosis of *CLN3*-disease in 6-18 weeks after their first

160 visit (mean: 10.7 weeks). They were referred with poor visual acuity, with all having

161 experienced a period of rapid visual decline before their referral to our tertiary center,

162 ranging from one to eighteen months in duration. Mean visual acuity (±SD, range) at disease

163 onset was 0.44 LogMAR (±0.44, 0.20-1.78 LogMAR). Mean visual acuity (±SD, range) by the

164 time of diagnosis was 1.34 LogMAR (±0.61, 0.30 LogMAR - light perception). The age of

165 disease onset ranged from 3 to 7 years (mean age 5.3 years). The time from disease onset to

166   diagnosis ranged from 1.5 to 5 years (mean time 2.9 years). Age at diagnosis of JNCL ranged

167   from 7 to 10 years (mean age 8.3 years). The medical history prior to first presentation in

168   five children was unremarkable (n=5, 62.5%), one patient had speech delay and learning

169   difficulties, and a further patient had been hospitalised aged 8 weeks with hypoglycaemia

170   and low cortisol. **Table 1** summarizes the clinical findings.

171   Six out of eight children were seen by an ophthalmologist at their local hospital prior

172   to referral to our tertiary center (n=6, 75%). The other two cases (cases 6 and 7) were

173   referrals from an orthoptist and General Practitioner respectively. In three cases (n=3,

174   37.5%, Cases 2, 5 and 7) legal guardians had reported concerns about vision from as early as

175   3 years of age (range 3 to 7). In two cases (Cases 2 and 4), teachers had reported visual

176   disturbance. At the time of referral, the presumed diagnoses in the eight cases were

177   Stargardt disease (n=1), severe retinal dystrophy (n=3), and unexplained visual loss (n=4)

178   (**Table 1**).

179   Of note, 6 out of 8 patients had eccentric fixation/'overlooking' (75%) either on

180   observation or on directed history. On directed detailed history, 6 out of 8 patients had

181   cognitive or neurological signs (75%) - including change in mood, behaviour, balance, or

182   memory. MRI was carried out in three children and was unremarkable.

183

184   *Retinal Imaging*

185   As shown in **Figures 1** and **3**, all but one patient (case 7) presented with a bull's-eye

186   maculopathy. Optic disc pallor, arteriolar attenuation, and subtle granularity of the RPE was

187   observed in all cases. Case 4 also developed inferior peripheral exudation, in keeping with a

188   Coats-like vasculopathy (not previously reported in JNCL), which spontaneously improved

9

189   over 12 months (**Figures 1 and 3**); and a mild mid-peripheral pigmentary retinopathy with

190   bone spicule formation.

191   Macular FAF images (**Figure 2**) depict marked foveal hypoautofluorescence with

192   varying degrees of surrounding diffuse reduction in macular autofluorescence in all patients

193   (n=8, 100%). In addition, a perifoveal ring of increased autofluorescence was present in

194   cases 3 and 6. Peripheral autofluorescence was variably decreased among the patients;

195   ranging from mildly diffuse hypoautofluorescence (cases 3, 5 and 6), to markdly diffuse

196   hypoautofluorescence (case 4). Case 1, 2, 7, and 8 show variable extend of decrease

197   autofluorescence between the two aforementioned groups. In cases 1 and 7, mild RPE

198   mottling was seen in the periphery (**Figure 2**). In case 4, striae of decreased signal were

199   observed in the periphery and perifoveal area (**Figure 2**).

200   OCT was available for analysis in 7 cases. In all cases OCT imaging revealed near

201   complete loss of photoreceptor cells, atrophy of the outer nuclear layer, outer plexiform

202   layer, and marked atrophy of the nerve fibre and ganglion cell layers (**Figure 3**). The ellipsoid

203   zone was markedly disrupted/absent, and it was difficult to identify remnants of the

204   photoreceptor layer, due to debris. Hyper-reflective dots were visible at the level of the

205   expected photoreceptor layer (**Figure 3**).

206   Mean subfoveal choroidal thickness was within age-adjusted normal limits, (mean

207   336 µm right eye and 330 µm left eye). Automated segmentation of the mGCL was

208   performed in four patients (Cases 1, 3, 4 and 6). The values obtained from the 1 mm

209   diameter central subfield area were excluded from analysis as the mGCL in the central

210   subfield was very thin, precluding adequate segmentation. The values corresponding to the

211   6mm outer ring were excluded as they fell outside the scanning area due to eccentric

212   fixation. The average mGCL of the intermediate 3mm ring was 10.84 μm (SD: ±2.87 μm)

213   (**Supplementary Figure 1**). The average mGCL thickness was 44.1 μm ± 9.22 μm, with mean

214   (5th-95th percentile) normative value for children 5-17 years (n=276) being 51.6 μm (44.43-

215   58.25 μm).[33]

216   In addition to mGCL thinning, changes at the level of nerve fiber layer (NFL) and

217   internal limiting membrane (ILM) were observed in all patients. Radial retinal striae were

218   observed within the vascular arcades in five cases (n=5, 62.5%, **Figures 3 and 4**). Striae

219   (folds) resembling epiretinal membranes, but without vessel alterations, were seen on

220   fundoscopy and color fundus photography (**Figure 4** - Case 2). No definite membrane was

221   seen joining the tips of the folds on OCT (**Figure 4**, Cases 1, 5, 7 and 8). In contrast, gliosis of

222   the inner retina, presented as increased reflectivity at the ILM,[34] was evident in all but one

223   patient (case 3). An increased, patchy (linear) signal observed at the level of the ILM with

224   severe disruption of the NFL, appears to have led to more prominent "folding" nasally,

225   possibly related to greater NFL thickness (**Figure 3**). Foci of increased signal, instead of

226   patchy linear areas, were observed in the three cases without folds (**Figure 4**, Cases 3, 4 and

227   6). The external limiting membrane (ELM) was present, however disrupted (**Figure 3**), and

228   no folds were present in these patients, perhaps representing an earlier stage of the

229   disease. The mean age at the time of OCT imaging was 8.9 years for patients with striae and

230   8.0 years for patients without striae.

231

232   *Electrophysiological Assessment*

233   Full-field and flash ERGs were recorded in all patients under photopic and scotopic

234   conditions. Cases 1, 2, 4 and 5 had undetectable ERGs, in keeping with severe rod and cone

235   photoreceptor dysfunction (**Figure 5A**). Cases 3, 6, 7 and 8 had undetectable scotopic dim

11

236   flash ERGs; strong flash ERGs were electronegative but with additional a-wave reduction.

237   The photopic single flash ERGs had a low b:a ratio but with additional a-wave reduction in

238   cases 7 and 8. The LA 30Hz flicker ERGs were mildly delayed in all cases with a detectable

239   response (cases 3, 6, 7 and 8) (**Figure 5A and 5B**). The findings were consistent with marked

240   generalised inner retinal dysfunction of rod (cases 3, 6, 7 and 8) and cone (cases 7 and 8)

241   systems, with additional rod and cone photoreceptor involvement in all cases. Pattern ERGs

242   were undetectable in the six cases tested in keeping with severe macular dysfunction.

243

244   *Blood film Microscopy/ Electron Microscopy*

245   Blood film microscopy performed for all eight patients demonstrated vacuolated

246   lymphocytes. Electron microscopy was done sequentially in seven patients and all showed

247   lysosomal (fingerprint) inclusions.

248

249

250

251   *Molecular Genetics*

252   All patients were molecularly confirmed as harboring likely disease-causing variants in *CLN3*.

253   Six out of eight patients were homozygous for the common 1.02kb deletion. Case 8 was

254   homozygous for c.(962+dup), case 7 was compound heterozygotes for c.(1056+3A>C) and

255   deletion of exon 2-5. One patient (case 3) was referred initially with 'molecularly confirmed'

256   Stargardt   disease   for   consideration   of   clinical   trials/studies.   The   clinical

257   presentation/detailed history/imaging was not in keeping with Stargardt disease and so

258   investigation was initiated for JNCL. The previously identified compound heterozygous

259   *ABCA4* variants were further assessed *in silico*, with one of the variants determined to be

260 unlikely to be pathogenic. Determination of disease-causation of *ABCA4* variants is highly

261 challenging given the vast allelic heterogeneity and highly polymorphic nature of this large

262 gene.

263

264 **Discussion**

265 This report characterizes the early retinal phenotype of juvenile Batten disease, highlights

266 the importance of early diagnosis of *CLN3* disease in young children who present with rapid

267 visual loss, with or without the presence of neurological or cognitive symptoms, and

268 describes conditions that can masquerade as *CLN3* disease.

269 Our case series identified a significant delay in diagnosis in all 8 children, with an

270 average delay of 2.9 years from first presentation to diagnosis, in line with previous studies

271 reporting a delay of 1.3 to 4 years.[25] [9] It is of note that in the past, the diagnosis was often

272 only made after the onset of seizures despite prior visual failure;[26] whereas, early diagnosis

273 should now be possible following the advancements in retinal imaging and molecular testing

274 that are now readily available.

275 There are several clinical symptoms (likely to require a directed careful history –

276 including eccentric viewing and changes in mood/behaviour/cognition/memory), and signs

277 on examination/detailed imaging, that should warrant directed investigations to promptly

278 diagnose *CLN3*-JNCL. These include visual loss, which is characteristically rapid, and was

279 present in all of our cases; most commonly reported in the literature between 6 to 8 years

280 of age.[9, 11, 25, 28] Other associated behavioural and cognitive impairments were also present

281 in six out of eight cases, however these were often not identified at the time of visual

282 complaints and / or not investigated or considered pertinent to the unexplained/otherwise

283 explained visual loss – thereby further contributing to delayed diagnosis.

284 Fundus abnormalities seen in *CLN3* disease such as "bulls-eye" maculopathy, retinal

285 vascular attenuation, and optic disc pallor were present in our series, however, these are

286 also features of other severe retinopathies.[23, 24] Previously, eccentric fixation or

287 "overlooking" has been attributed to a degree of superior peripheral retinal sparing.[26]

288   Despite the majority of the patients in our study having eccentric fixation/overlooking

289   (**Table 1**), the disease appeared relatively symmetrical between the superior and inferior

290   retina on fundus autofluorescence imaging (**Figure 3**); suggesting no obvious anatomical

291   difference and also no functional difference (indirectly) – although, we cannot exclude that

292   *direct* functional testing may identify a difference between superior and inferior retinal

293   sensitivity.

294   Abnormalities in OCT features can be very helpful in guiding the clinician to directly

295   investigate *CLN3*-disease; including the profound degree and extent of outer retinal loss of

296   lamination at a relatively young age, significant inner retinal thinning, and also the presence

297   of increased inner retinal reflectivity. The increased reflectivity has been described as being

298   secondary to epiretinal membrane (ERM) formation in several reports. Haisworth et al,

299   identified ERM in 33% of their cohort (n=24), based on fundus appearance alone.[21] More

300   recently, Dulz et al described a striation pattern without ERM in all their patients (n=11,

301   mean age 14.4 years), using OCT.[9] In our cohort, all patients had reflectivity changes in the

302   nerve fibre layer (NFL) and ILM. Although the mean age of our cohort was lower (average

303   age 8.9 yrs), retinal striation was observed in 62.5% of the patients – distinct from typical

304   ERM; with the three patients without striae being on average a year younger (8 years)

305   (**Figure 4**). Our findings of profound diffuse macular ganglion cell thinning are in keeping

306   with the degenerative NFL and mGCL loss reported in histological studies.[35, 36]

307   The scotopic ERGs in four of four cases with a detectable response had

308   electronegative waveforms, consistent with dysfunction that is post-phototransduction or

309   inner retinal, but with a-wave reduction indicating significant additional loss of

310   photoreceptor function. An electronegative ERG has often been associated with juvenile

311   *CLN3* disease and may prompt screening in some cases, particularly if the photopic ERG

312 shows a reduced b:a ratio.[25] It is noted however that an electronegative ERG is not

313 diagnostic and is a feature of congenital stationary night blindness, X-linked retinoschisis

314 and many other disorders.[22, 37-39]

315   One patient was referred initially with 'molecularly confirmed' Stargardt disease

316 (STGD) for consideration of clinical trials/studies. The clinical presentation/detailed

317 history/imaging was not entirely typical of STGD and so investigation was initiated for JNCL.

318 The previously identified compound heterozygous *ABCA4* variants were further assessed *in*

319 *silico*, with one of the variants determined to be unlikely to be pathogenic. Determination of

320 disease-causation of *ABCA4* variants is highly challenging given the vast allelic heterogeneity

321 and highly polymorphic nature of this large gene. This case highlights (i) that the clinician

322 needs to be mindful that severe *ABCA4*-retinopathy associated with generalised cone-rod

323 dystrophy at an early age can masquerade as *CLN3*-JNCL, (ii) the difficulties in definitively

324 ascribing disease-causation to identified sequence variants in this era of genomic

325 ophthalmology and more readily-accessible genetic testing, and (iii) further illustrates the

326 challenges in diagnosing *CLN3* disease in a timely fashion and the potential consequences of

327 mistaken diagnosis.

328   Early diagnosis of JNCL remains a diagnostic challenge, particularly as other severe

329 retinal dystrophies can present with early onset visual loss. Moreover, associated non-

330 ocular symptoms/signs are often compartmentalised and investigated separately which can

331 lead to further delay. We suggest that a child with bilateral rapidly progressive vision loss,

332 with or without cognitive/behavioural problems at presentation, should have microscopy of

333 a peripheral blood film to detect the presence of vacuolated lymphocytes, which can act as

334 a sensitive screening test (all patients with *CLN3* disease will test positive); followed by

16

335   electron microscopy for storage (fingerprint) inclusions.[15] Diagnostic confirmation should be

336   done with molecular genetic screening of *CLN3* (**Figure 6**).

337   The most common variant in *CLN3*-JNCL is a 1kb deletion resulting in a frameshift

338   and a truncated protein product.[10] In our cohort, 75% of cases were homozygous for this

339   deletion and had similar clinical presentations. Case 8, who harbored the c.(962+dup)

340   variant homozygously was reported to have better VA at presentation, but by the time of

341   diagnosis had similar VA to the other patients. Case 7, the only compound heterozygote in

342   our cohort (c.(1056+3A>C) and deletion of exon 2-5) had a milder ocular phenotype, with

343   the most preserved VA in the cohort and a degree of residual ellipsoid zone on OCT (**Figure**

344   **3**). As this patient presented with early cognitive and behavioural abnormalities, it could be

345   speculated that this genetic variant may have less deleterious effects on vision. Case 7 also

346   had electronegative ERGs but with an altered waveform morphology of the rod ERG, which

347   was not observed in any of the other subjects. The significance of this ERG finding is

348   uncertain.   Although there is no treatment that has yet been shown in a clinical trial to

349   benefit patients with JNCL, it is important to explain the genetics of the disease to the

350   parents, provide genetic counselling, offer to follow the child yearly for routine eye care,

351   and offer to refer them to a pediatric neurologist, knowledgeable pediatrician, or family

352   practitioner who is willing and able to help follow and care for the child. This includes

353   specialist knowledge of certain medications that are more likely to induce adverse side

354   effects when given to a child with JNCL. Referral to international foundations that support

355   research on the NCL disorders, social workers, or local or national support groups of parents

356   who have children with JNCL may help parents and families cope with issues commonly

357   seen as the disease progresses.

358   To date, there are no treatments available for juvenile *CLN3* Batten disease or other

359 forms of NCL. The majority of studies has focused on developing therapeutic interventions

360 to combat the neurodegeneration in NCL, including enzyme replacement therapy, gene

361 therapy, stem cell transplantation and pharmacological approaches.[40, 41] Most notably, *CLN2*

362 disease patients that received biweekly intraventricular infusion of soluble CLN2 enzyme

363 (NCT01907087, NCT02485899) showed no significant decline in motor or language skills and

364 overall disease progression was considerably slowed during the reporting period.[41] The

365 treatment has now received FDA and EMA approval. A phase I/II trial has also started for

366 *CLN6* disease using gene therapy administered by a single intrathecal injection of adeno-

367 associated virus (AAV) 2/9 carrying *CLN6* (NCT02725580). This study is on-going, but data

368 from 8 out of 12 patients two years post vector injection are available and show promising

369 preliminary results. Based on these data, a phase I/II clinical trial has started recruiting for

370 *CLN3* disease, to investigate intrathecally administered AAV2/9-*CLN3* (NCT037770572).

371 Although, these studies will primarily assess treatment safety and effects on neurological

372 features, they may also help to determine whether brain-directed gene therapy has any

373 impact on vision in *CLN6* and *CLN3* patients. As *CLN6* and *CLN3* encode membrane-bound

374 proteins that are not passed on to neighbouring cells, it is more likely that gene therapy

375 directly targeting the eye will be more effective to prevent retinal degeneration in both

376 diseases. A proof-of-concept study demonstrated that ocular gene therapy is therapeutic in

377 *Cln6^{nclf}* mice, a mouse model for *CLN6* disease, when the inner retina was treated.[41]

378 Preclinical ocular gene therapy for *CLN3* disease has not been described yet. However, a

379 similar gene therapy approach targeting the cells of the inner retina as used in *Cln6^{nclf}* mice

380 could also be effective in *Cln3*-deficient mice;[25] and may also be relevant to human *CLN3*

381 disease (both syndromic and non-syndromic).

18

382   Herein, we have described cases of juvenile *CLN3* disease in detail, highlighting

383 delayed/mistaken diagnosis, diagnostic challenges, providing diagnostic insights, novel

384 observations and recommendations, and also highlighting the latest clinical research and

385 on-going/planned clinical trials. We have also emphasized of role of the ophthalmologist,

386 and paediatrician or primary care provider and the need for additional continued support

387 for the family. Whilst timely diagnosis of JNCL is often challenging, given the rapidly

388 progressive and unfavourable prognosis of the disease, early diagnosis is important both to

389 provide timely clinical management and support, and to facilitate access to novel

390 therapeutic interventions at the early disease stages.

391

392 **LEGENDS**

393 **Figure 1. Clinical features on color fundus photography.**

394 Color fundus photographs of five cases with juvenile neuronal ceroid lipofuscinosis;

395 depicting optic disc pallor, macular atrophy with subtle granularity of the retinal pigment

396 epithelium (RPE) and retinal arteriolar attenuation. Note the pigmentary changes

397 reminiscent of bone spicules and unilateral Coats-like reaction in case 4. The second row for

398 case 4 shows the exudation at baseline and its improvement over a follow-up period of 12

399 months.

400

401 **Figure 2. Fundus autofluorescence findings.**

402 Fundus autofluorescence images showing marked foveal hypoautofluorescence with varying

403 degrees of surrounding diffuse reduction in macular autofluorescence. Cases **3** and **6:** A ring

404 of increased autofluorescence (white arrow heads). Cases **3, 5** and **6** show mild diffuse

405 peripheral hypoautofluorescenceand, case **4** shows advanced diffuse hypoautofluorescence.

406 Case 1, 2, 7, and 8 show variable extend of decrease autofluorence between the two

407 aforementioned groups.

408

409 **Figure 3. Optical coherence tomography findings**.

410 Spectral-domain optical coherence tomography (SD-OCT) macular scans for all patients in

411 the cohort, at the time of diagnosis, depicting significant macular atrophy with almost

412 complete loss of the ellipsoid zone, hyper-reflective dots at the outer retinal level, marked

413 atrophy of the outer nuclear layer, outer plexiform layer, ganglion cell layer and nerve fibre

414 layer. Glial fibrosis is observed at the level of the inner retina. The white arrow heads mark

415 possible areas of residual ellipsoid zone. The orange arrow heads mark an a example of

416 continuous, even though alter, external limiting membrane, despite the excessive loss of the

417 photoreceptor layer. The white borders delineate regions of interest shown in greater

418 magnification in Figure 4.

419

420

421 **Figure 4: Macular striation and degenerative changes**

422 Striation and/or degenerative changes were present in all patients. High magnification of

423 the marked areas in **Figure 3** are shown, from horizontal OCT scans of the nasal fovea.

424 Retinal radial striae within the vascular arcades were observed in cases 1, 5, 7 and 8. Striae,

425 resembled the appearance of epiretinal membranes on fundoscopy and color fundus

426 photography, but no vessel alterations are seen and no definite membrane observed joining

427 the tips, marked with white arrow heads, of the folds seen on OCT. Foci of increased signal,

428 marked with yellow arrow heads, were observed in Case 3, 4 and 6 who did not have folds.

429 In contrast to case with folds, where the areas of increase signal were greater in size and

430 had a more linear distribution.

431

432 **Figure 5: Electroretinography**

433 Electroretinography recorded with lower eyelid skin electrodes in cases 4, 5, 6 and 8 (A) and

434 with corneal electrodes in case 7 (B). Note 20ms pre-stimulus delay in single flash ERGs.

435 Electrode-specific control recordings are shown for comparison but without a 20ms pre-

436 stimulus delay in B. ISCEV-standard stimuli were used in case 4 (without mydriasis) and in

437 cases 6 and 7; a strobe was used to deliver flashes in subjects unable to comply with

438 Ganzfeld testing (dim flash rod ERG/DA0.01 ERG excluded from the protocol). ISCEV

439   standard testing (cases 6 and 7) included the dark-adapted (DA) ERGs (flash strengths 0.01

440   and 10.0 cd.s/m2; DA 0.01 and DA 10.0) and light-adapted (LA) ERGs for a flash strength of

441   3.0 cd.s/m2 (LA 3.0; 30Hz and 2Hz). Data are shown for one eye but all had symmetrical

442   responses. Broken lines replace blink/eye movement artefacts occurring after ERG b-waves

443   for clarity. Recordings from patients are superimposed to demonstrate reproducibility. Note

444   small differences in scaling and format of skin ERGs (A) related to use of different recording

445   equipment. See text for ERG analysis.

446

447   **Figure 6: Diagnostic algorithm for juvenile neuronal ceroid lipofuscinosis (JNCL), *CLN3*-**

448   **associated disease.**

449   In a child with bilateral rapidly progressive vision loss, microscopy of peripheral blood film

450   can detect the presence of vacuolated lymphocytes, a sensitive screening test for JNCL,

451   followed by electron microscopy for lysosomal storage inclusions. Confirmation of the

452   diagnosis should follow with molecular genetic testing for *CLN3* variants.

453

454   **FOOTNOTES**

455

REFERENCES

1. Johnson TB, Cain JT, White KA, et al. Therapeutic landscape for Batten disease: current treatments and future prospects. Nat Rev Neurol 2019;15(3):161-78.
2. Isolation of a novel gene underlying Batten disease, CLN3. The International Batten Disease Consortium. Cell 1995;82(6):949-57.
3. Williams RE, Mole SE. New nomenclature and classification scheme for the neuronal ceroid lipofuscinoses. Neurology 2012;79(2):183-91.
4. Licchetta L, Bisulli F, Fietz M, et al. A novel mutation af Cln3 associated with delayed-classic juvenile ceroid lipofuscinois and autophagic vacuolar myopathy. Eur J Med Genet 2015;58(10):540-4.
5. Mole SE, Williams RE. Neuronal Ceroid-Lipofuscinoses. In: Adam MP, Ardinger HH, Pagon RA, et al., eds. GeneReviews((R)). Seattle (WA): University of Washington, Seattle
University of Washington, Seattle. GeneReviews is a registered trademark of the University of Washington, Seattle. All rights reserved., 1993.
6. Schultz ML, Tecedor L, Chang M, Davidson BL. Clarifying lysosomal storage diseases. Trends Neurosci 2011;34(8):401-10.
7. Mink JW, Augustine EF, Adams HR, et al. Classification and natural history of the neuronal ceroid lipofuscinoses. J Child Neurol 2013;28(9):1101-5.
8. Mole SE. The genetic spectrum of human neuronal ceroid-lipofuscinoses. Brain Pathol 2004;14(1):70-6.
9. Dulz S, Wagenfeld L, Nickel M, et al. Novel morphological macular findings in juvenile CLN3 disease. Br J Ophthalmol 2016;100(6):824-8.
10. Jarvela I, Autti T, Lamminranta S, et al. Clinical and magnetic resonance imaging findings in Batten disease: analysis of the major mutation (1.02-kb deletion). Ann Neurol 1997;42(5):799-802.
11. Mole SE, Williams RE, Goebel HH. Correlations between genotype, ultrastructural morphology and clinical phenotype in the neuronal ceroid lipofuscinoses. Neurogenetics 2005;6(3):107-26.
12. Ku CA, Hull S, Arno G, et al. Detailed Clinical Phenotype and Molecular Genetic Findings in CLN3-Associated Isolated Retinal Degeneration. JAMA Ophthalmol 2017;135(7):749-60.
13. Santavuori P. Neuronal ceroid-lipofuscinoses in childhood. Brain Dev 1988;10(2):80-3.
14. Kousi M, Lehesjoki AE, Mole SE. Update of the mutation spectrum and clinical correlations of over 360 mutations in eight genes that underlie the neuronal ceroid lipofuscinoses. Hum Mutat 2012;33(1):42-63.
15. Anderson G, Smith VV, Malone M, Sebire NJ. Blood film examination for vacuolated lymphocytes in the diagnosis of metabolic disorders; retrospective experience of more than 2,500 cases from a single centre. J Clin Pathol 2005;58(12):1305-10.
16. Cialone J, Adams H, Augustine EF, et al. Females experience a more severe disease course in Batten disease. J Inherit Metab Dis 2012;35(3):549-55.
17. Marshall FJ, de Blieck EA, Mink JW, et al. A clinical rating scale for Batten disease: reliable and relevant for clinical trials. Neurology 2005;65(2):275-9.
18. Ostergaard JR. Juvenile neuronal ceroid lipofuscinosis (Batten disease): current insights. Degener Neurol Neuromuscul Dis 2016;6:73-83.

508   19.   Eksandh LC, Ponjavic V, Ayyagari R, et al. Phenotypic expression of juvenile
509   X-linked retinoschisis in Swedish families with different mutations in the XLRS1
510   gene. Arch Ophthalmol 2000;118(8):1098-104.
511   20.   Bensaoula T, Shibuya H, Katz ML, et al. Histopathologic and
512   immunocytochemical analysis of the retina and ocular tissues in Batten disease.
513   Ophthalmology 2000;107(9):1746-53.
514   21.   Hainsworth DP, Liu GT, Hamm CW, Katz ML. Funduscopic and angiographic
515   appearance in the neuronal ceroid lipofuscinoses. Retina 2009;29(5):657-68.
516   22.   Horiguchi M, Miyake Y. Batten disease--deteriorating course of ocular
517   findings. Jpn J Ophthalmol 1992;36(1):91-6.
518   23.   Krohne TU, Herrmann P, Kopitz J, et al. [Juvenile neuronal ceroid
519   lipofuscinosis. Ophthalmologic findings and differential diagnosis]. Ophthalmologe
520   2010;107(7):606-11.
521   24.   Bozorg S, Ramirez-Montealegre D, Chung M, Pearce DA. Juvenile neuronal
522   ceroid lipofuscinosis (JNCL) and the eye. Surv Ophthalmol 2009;54(4):463-71.
523   25.   Collins J, Holder GE, Herbert H, Adams GG. Batten disease: features to
524   facilitate early diagnosis. Br J Ophthalmol 2006;90(9):1119-24.
525   26.   Spalton DJ, Taylor DS, Sanders MD. Juvenile Batten's disease: an
526   ophthalmological assessment of 26 patients. Br J Ophthalmol 1980;64(10):726-32.
527   27.   Weleber RG. The dystrophic retina in multisystem disorders: the
528   electroretinogram in neuronal ceroid lipofuscinoses. Eye (Lond) 1998;12 (Pt
529   3b):580-90.
530   28.   Mantel I, Brantley MA, Jr., Bellmann C, et al. Juvenile neuronal ceroid
531   lipofuscinosis (Batten disease) CLN3 mutation (Chrom 16p11.2) with different
532   phenotypes in a sibling pair and low intensity in vivo autofluorescence. Klin Monbl
533   Augenheilkd 2004;221(5):427-30.
534   29.   Autti TH, Hamalainen J, Mannerkoski M, et al. JNCL patients show marked
535   brain volume alterations on longitudinal MRI in adolescence. J Neurol
536   2008;255(8):1226-30.
537   30.   McCulloch DL, Marmor MF, Brigell MG, et al. ISCEV Standard for full-field
538   clinical electroretinography (2015 update). Doc Ophthalmol 2015;130(1):1-12.
539   31.   Holder G, Robson A. Paediatric electrophysiology: a practical approach .
540   Essentials in Ophthalmology, Ed Lorenz B Springer-Verlag, Berlin 2006:133-55.
541   32.   Bach M, Brigell MG, Hawlina M, et al. ISCEV standard for clinical pattern
542   electroretinography (PERG): 2012 update. Doc Ophthalmol 2013;126(1):1-7.
543   33.   Yoo YJ, Hwang JM, Yang HK. Inner macular layer thickness by spectral
544   domain optical coherence tomography in children and adults: a hospital-based study.
545   Br J Ophthalmol 2019.
546   34.   Preising MN, Abura M, Jager M, et al. Ocular morphology and function in
547   juvenile neuronal ceroid lipofuscinosis (CLN3) in the first decade of life. Ophthalmic
548   Genet 2017;38(3):252-9.
549   35.   Traboulsi EI, Green WR, Luckenbach MW, de la Cruz ZC. Neuronal ceroid
550   lipofuscinosis. Ocular histopathologic and electron microscopic studies in the late
551   infantile, juvenile, and adult forms. Graefes Arch Clin Exp Ophthalmol
552   1987;225(6):391-402.
553   36.   Goebel HH, Fix JD, Zeman W. The fine structure of the retina in neuronal
554   ceroid-lipofuscinosis. Am J Ophthalmol 1974;77(1):25-39.
555   37.   Weleber RG, Gupta N, Trzupek KM, et al. Electroretinographic and
556   clinicopathologic correlations of retinal dysfunction in infantile neuronal ceroid
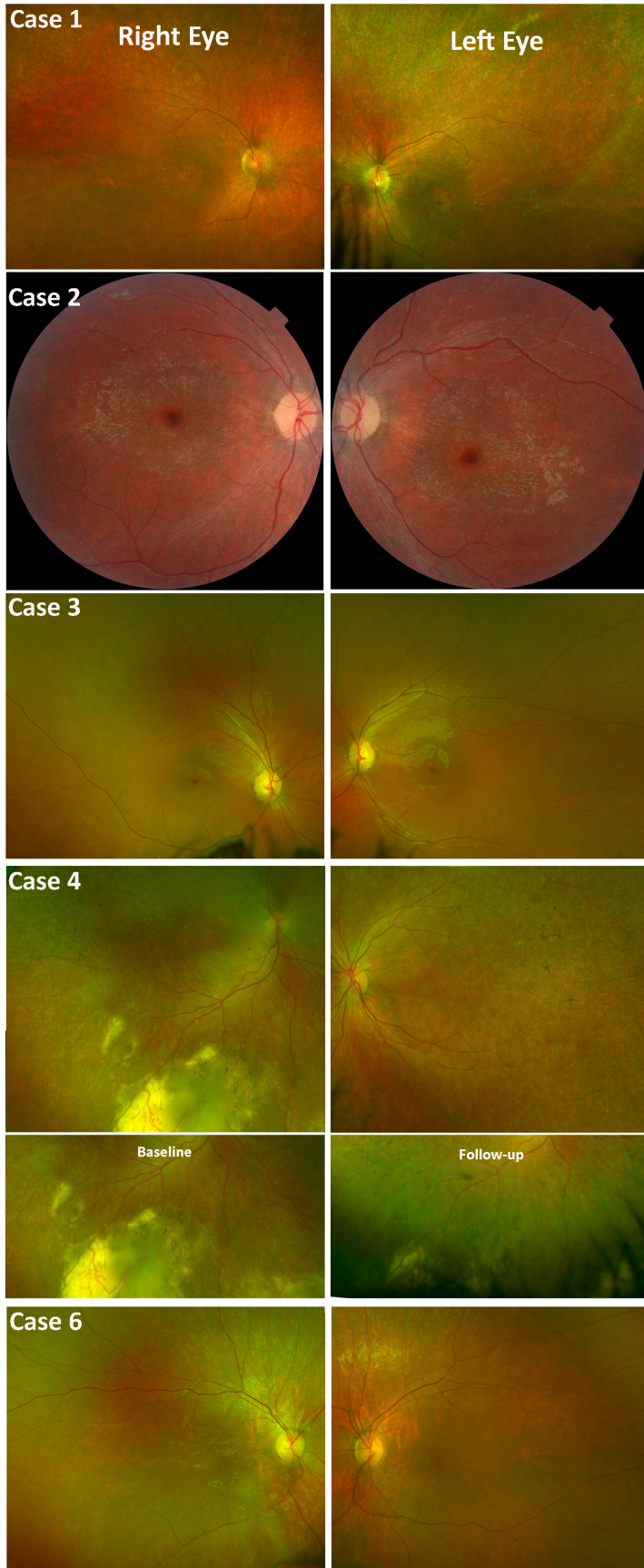557   lipofuscinosis (infantile Batten disease). Mol Genet Metab 2004;83(1-2):128-37.

558 38.   Audo I, Robson AG, Holder GE, Moore AT. The negative ERG: clinical
559 phenotypes and disease mechanisms of inner retinal dysfunction. Surv Ophthalmol
560 2008;53(1):16-40.
561 39.   Robson AG, Nilsson J, Li S, et al. ISCEV guide to visual electrodiagnostic
562 procedures. Doc Ophthalmol 2018;136(1):1-26.
563 40.   Mole SE, Anderson G, Band HA, et al. Clinical challenges and future
564 therapeutic approaches for neuronal ceroid lipofuscinosis. Lancet Neurol
565 2019;18(1):107-16.
566 41.   Schulz A, Ajayi T, Specchio N, et al. Study of Intraventricular Cerliponase Alfa
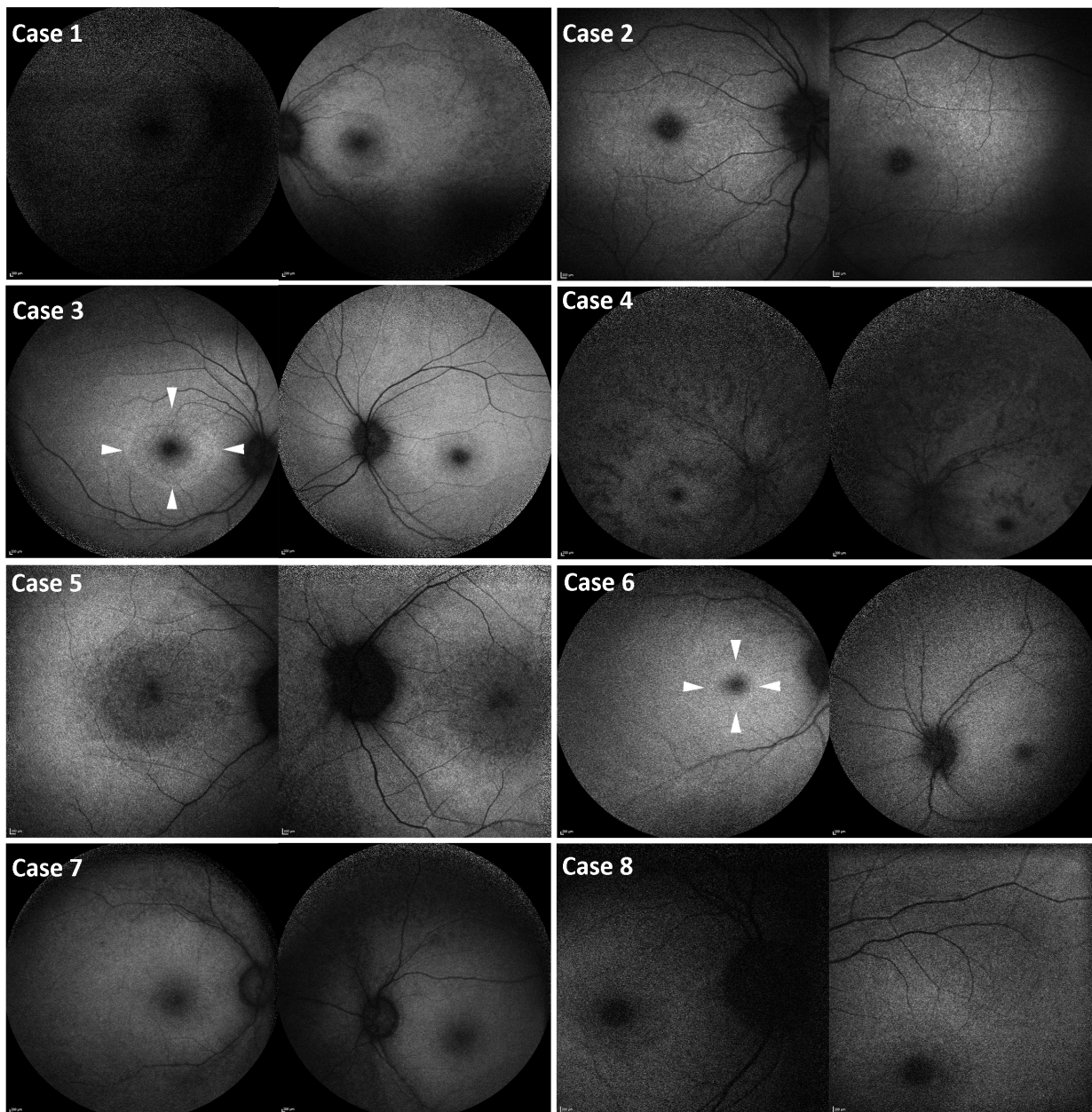567 for CLN2 Disease. N Engl J Med 2018;378(20):1898-907.
568

Table 1. Clinical features
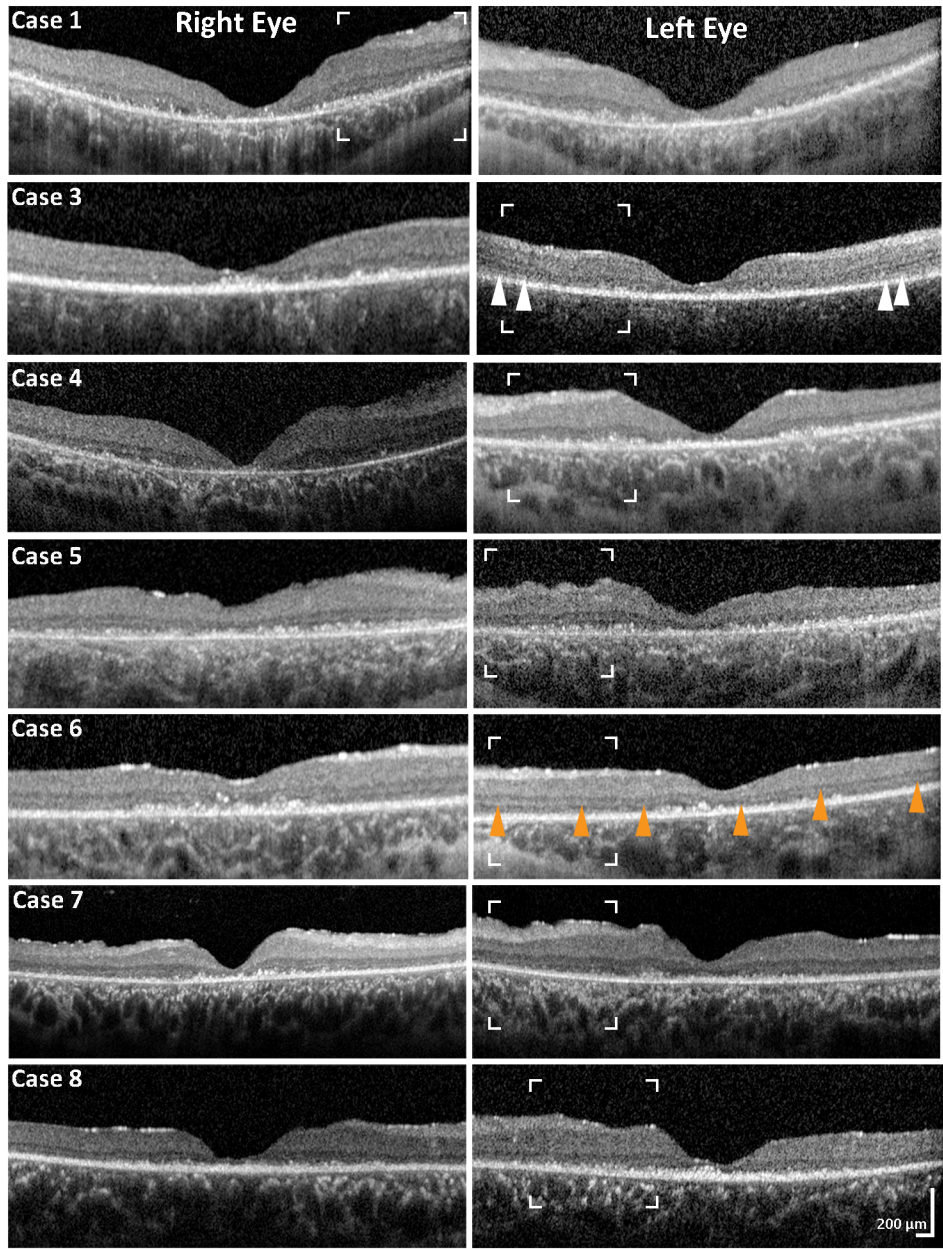
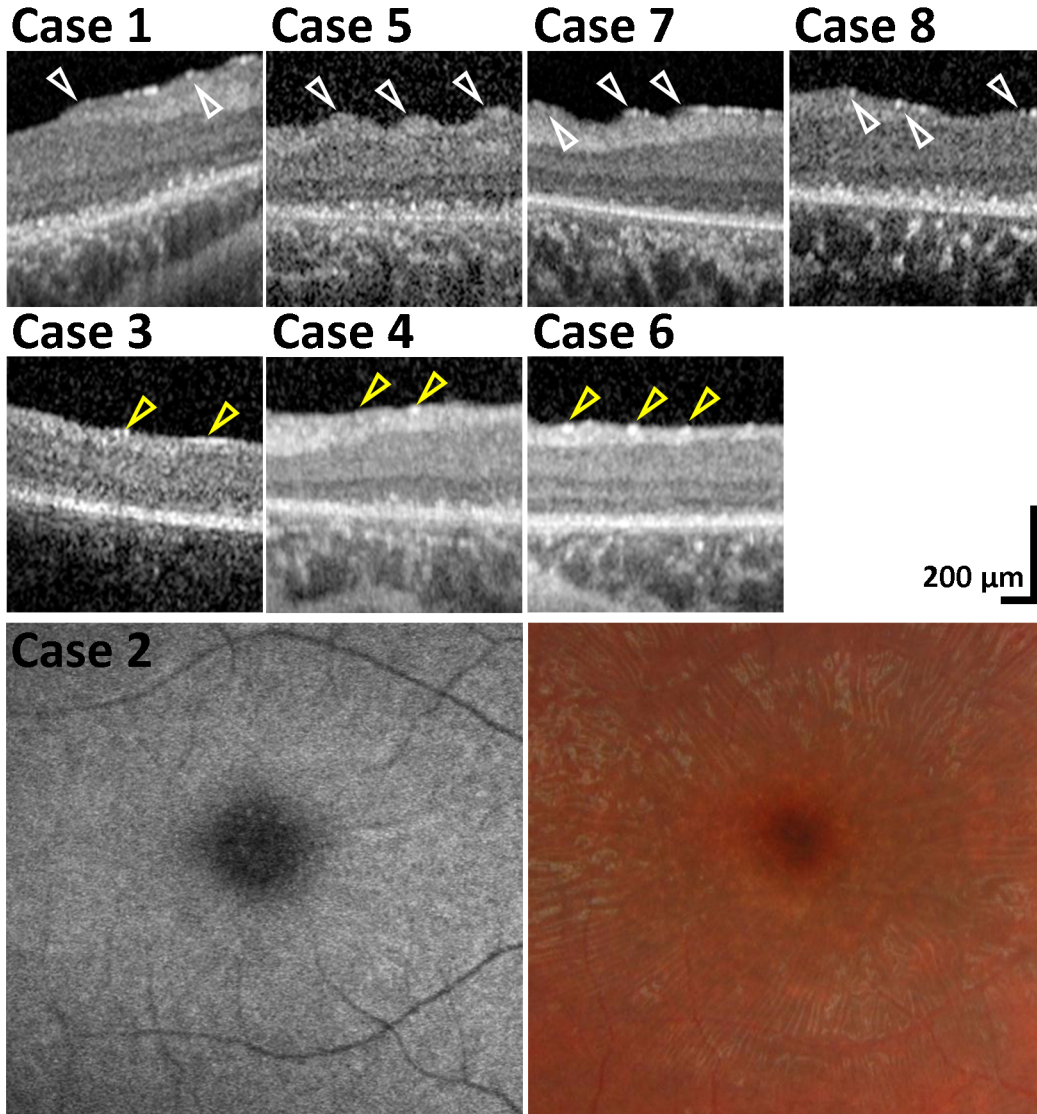|	Case 1	Case 2	Case 3	Case 4	Case 5	Case 6	Case 7	Case 8
Sex (F/M)	F	F	F	M	F	M	M	F
Age at onset (y)	5	5.5	3	7	4	6	6	6
Initial clinical findings at first evaluation:	Macular atrophy, retinal degeneration on OCT	Nystagmus, reduced vision, poor night vision	Foveal thinning, optic disc pallor, bull's-eye maculopathy, poor color vision/night vision	Bilateral macular changes, optic disc pallor	Visual impairment	Non correctable vision, poor color vision	Unexplained poor vision	Esotropia, left amblyopia
VA; R , L (LogMAR)	1.78 , 1.78	0.60 , 0.48	0.35 , 0.80	0.60 , 0.75	0.80 , 0.80	0.70 , 0.50	0.26 , 0.20	0.18 , 0.48
Neurological/ behavioural signs	Speech delay, 'clumsiness', seizures	None	Behavioural and cognitive decline (ASD?); 'clumsiness'	Emotional difficulties, cognitive decline	None	None	Behavioural decline	Speech and language delay
Rapid visual decline within:	6 months	1 month	12-18 months	1 year	12-18 months	1 year	1 year	1 year
Diagnosis on referral to MEH:	Severe retinal dystrophy	Severe retinal dystrophy	Molecularly confirmed Stargardt disease (ABCA4)	Severe retinal dystrophy	Unexplained vision loss	Unexplained vision loss	Unexplained vision loss	Unexplained vision loss
Age at Diagnosis (y):	10	7	8	9	9	7	8	8
Clinical features at time of diagnosis:	Profound macular atrophy, optic disc pallor, retinal vascular attenuation	Rotary nystagmus, pale optic discs, bull's-eye maculopathy, bilateral epiretinal membrane, retinal vascular attenuation	Profound loss of inner and outer retina, bilateral epiretinal membrane, bull's-eye maculopathy	Bilateral macular atrophy	Pale optic discs, attenuated vessels, bilateral macular atrophy	Loss of central retinal structure, bilateral epiretinal membrane, poor color /night vision, pale optic discs	Bilateral epiretinal membrane, outer retinal loss, pale optic discs	Bilateral macular atrophy, foveal sheen
VA; R , L (LogMAR)	PL, PL	1.35 , 1.60	1.20 , 1.30	1.0 , 1.10	1.30 , 1.23	1.20 ,1.20	0.50 , 0.30	1.30 , 1.30
Eccentric fixation/'overlooking'	✓	✓	✓	NR	NR	✓	✓	✓
Neurological /behavioural signs	Speech delay, clumsiness	None	Behavioural and cognitive decline, clumsiness	Cognitive decline	None	Clumsiness, memory loss, behavioural decline	Clumsiness, behavioural decline	Speech and language delay, poor concentration

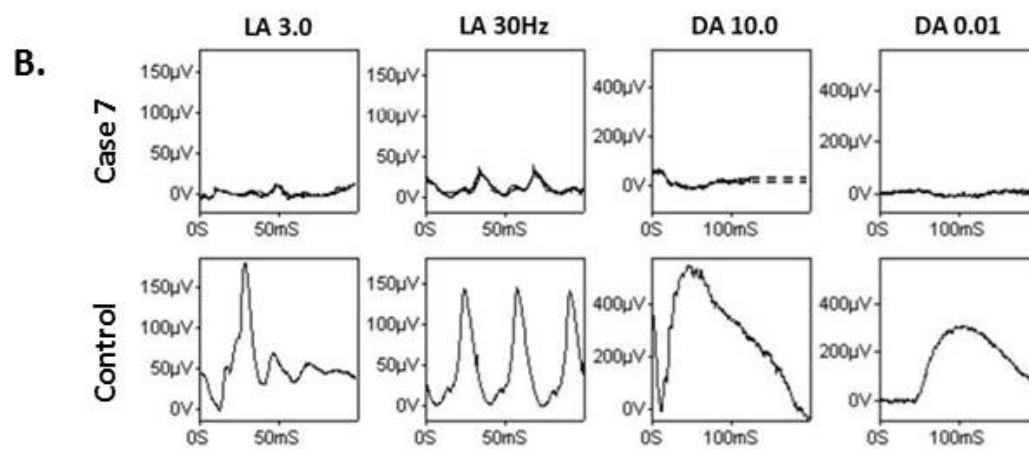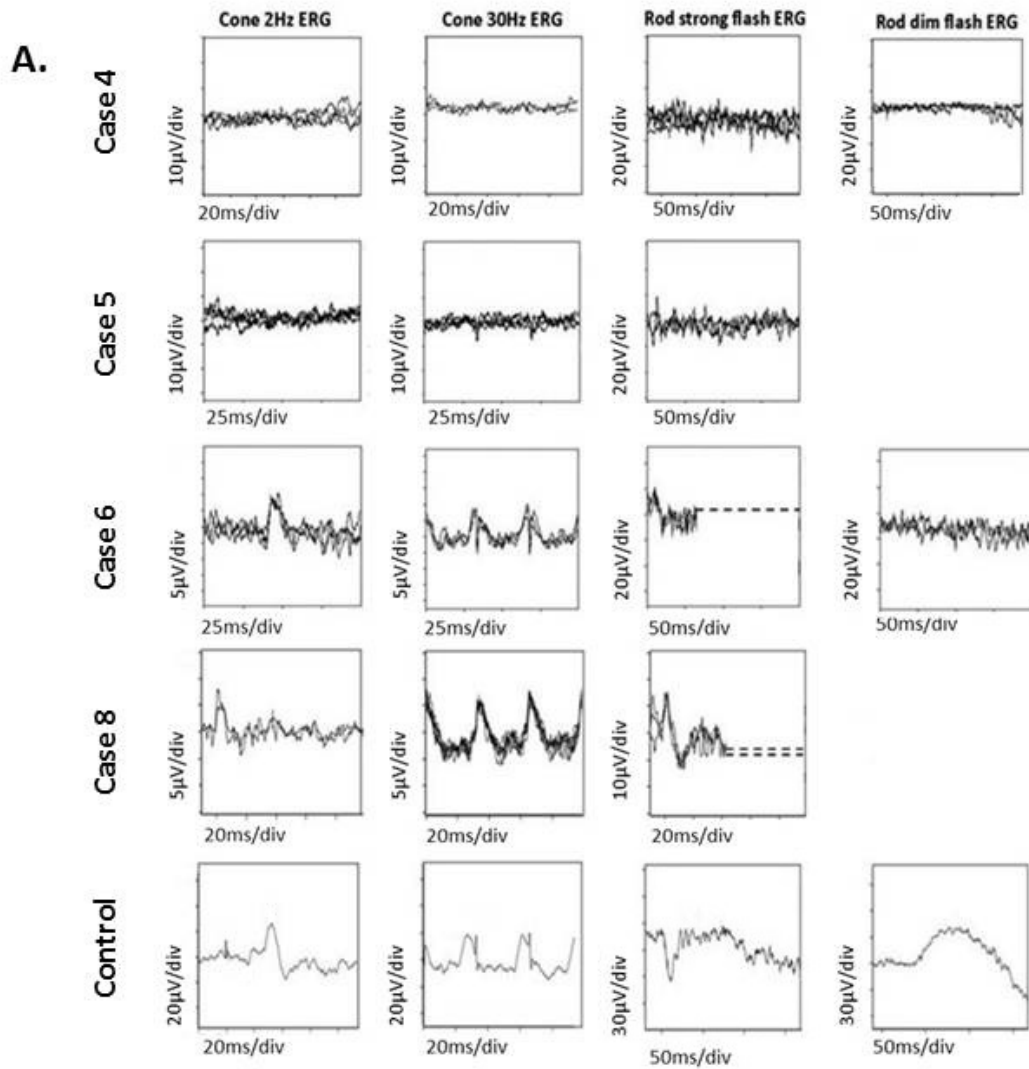ASD=Autistic spectrum disorder; NR = Not recorded; PL=Perception of light, R; Right Eye, L; Left Eye

Case 1 Right Eye Left Eye

Case 2

Case 3

Case 4

Baseline Follow-up

Case 6

Case 1 Case 5 Case 7 Case 8

Case 3 Case 4 Case 6

200 μm

Case 2

A.

| | Cone 2Hz ERG | Cone 30Hz ERG | Rod strong flash ERG | Rod dim flash ERG |

Case 4 — 10μV/div, 20ms/div; 10μV/div, 20ms/div; 20μV/div, 50ms/div; 20μV/div, 50ms/div

Case 5 — 10μV/div, 25ms/div; 10μV/div, 25ms/div; 20μV/div, 50ms/div

Case 6 — 5μV/div, 25ms/div; 5μV/div, 25ms/div; 20μV/div, 50ms/div; 20μV/div, 50ms/div

Case 8 — 5μV/div, 20ms/div; 5μV/div, 20ms/div; 10μV/div, 20ms/div

Control — 20μV/div, 20ms/div; 20μV/div, 20ms/div; 30μV/div, 50ms/div; 30μV/div, 50ms/div

B.

| | LA 3.0 | LA 30Hz | DA 10.0 | DA 0.01 |

Case 7 — 150μV, 100μV, 50μV, 0V / 0S 50mS; 150μV, 100μV, 50μV, 0V / 0S 50mS; 400μV, 200μV, 0V / 0S 100mS; 400μV, 200μV, 0V / 0S 100mS

Control — 150μV, 100μV, 50μV, 0V / 0S 50mS; 150μV, 100μV, 50μV, 0V / 0S 50mS; 400μV, 200μV, 0V / 0S 100mS; 400μV, 200μV, 0V / 0S 100mS

Ophthalmology

Child with rapidly progressive vision loss

± Cognitive/Behavioral /Mood Changes

± Retinal Imaging
± Electronegative ERG

Alternative Dx

Pathology

Peripheral Blood Film Microscopy

Vacuolated Lymphocytes

Electron Microscopy

Storage Lysosomal Inclusions

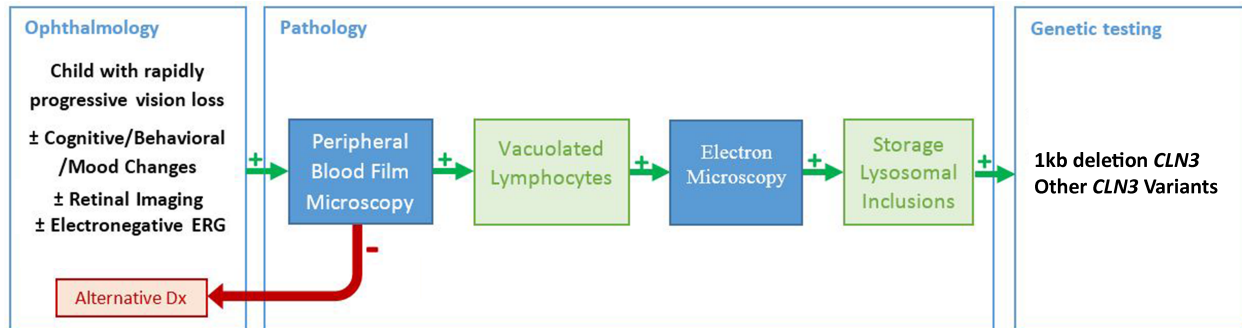**Genetic testing**

1kb deletion *CLN3*
Other *CLN3* Variants

Précis (Highlights)

This report highlights the importance of considering juvenile neuronal ceroid lipofuscinosis disease in young children who present with rapid visual loss, with or without the presence of neurological or cognitive symptoms.